Dyes and Pigments 132 (2016) 329–335

Contents lists available at ScienceDirect

Dyes and Pigments

journal homepage: www.elsevier.com/locate/dyepig

A fluorene-fused triphenodioxazine (FTPDO) based polymer with remarkable thermal stability and significantly enhanced charge transport performance in air

Libing Guo [a, 1], Jesse Quinn [b, 1], Jianli Wang [a], Chang Guo [b], Xu Li [a], Jinliang Wang [a, **], Yuning Li [a, b, *]

[a] Institute of Chemistry, Henan Academy of Sciences, 56 Hongzhuan Road, Jinshui District, Zhengzhou, Henan, 450002, China
[b] Department of Chemical Engineering and Waterloo Institute of Nanotechnology (WIN), University of Waterloo, 200 University Ave West, Waterloo, N2L 3G1, Canada

ARTICLE INFO

Article history:
Received 3 March 2016
Received in revised form
16 April 2016
Accepted 9 May 2016
Available online 12 May 2016

Keywords:
Triphenodioxazine
Polymer semiconductors
Thin film transistors
Solar cells
Printed electronics
Air-stable

ABSTRACT

We report the synthesis of a novel electron acceptor building block, fluorene-fused triphenodioxazine (**FTPDO**), and a donor-acceptor polymer based on **FTPDO** and bithiophene, **PFTPDOBT**. This new polymer possesses a narrow band gap (1.66 eV) with low-lying frontier energy levels and exhibits hole transport characteristics in organic thin film transistors (OTFTs). Thin films of **PFTPDOBT** show remarkable thermal stability in air at temperatures of up to 250 °C with no noticeable differences in UV–Vis absorption characteristics in comparison to the films annealed in nitrogen. Surprisingly, OTFTs with the polymer thin films annealed in air and measured in air outperform significantly the devices annealed and measured in nitrogen.

1. Introduction

Organic electronics are envisioned to have a broad range of applications being particularly relevant in such areas as displays, lighting, solar cells, intelligent packaging, smart labels, and sensors [1–6]. Organic electronics may be simply fabricated by cost effective printing techniques and have the ability to bow, curve, and attune to non-planar surfaces where inorganic materials simply cannot contend. Furthermore, organic electronics have the potential to interface with biological systems allowing for exciting new applications in fields such as medicine, environment, communication, and security. With the advent of high-performance organic thin film transistors (OTFTs), organic photovoltaics (OPVs), and other organic electronics that are comparable to their inorganic counterparts within the past few years, there has been a growing effort in academic and industrial research.

Many high-performance small molecule and polymer semiconductors have originated from the core building blocks of some commonly used dyes and pigments such as diketopyrrolopyrrole (DPP) (the core structure of Pigment Red 254) [5,6], indigo (ID) [7–10], and isoindigo (ID) [11–13]. With established synthetic procedures for these dyes and pigments lower cost manufacturing is possible. More importantly, the remarkable environmental stability of these compounds makes them ideal for the development of air-stable organic semiconductors and devices. A common feature for these high-performing building blocks is that they all contain large fused conjugated ring structures, which allow for highly effective π-electron delocalization and large intermolecular π-π overlapping, both of which are essential for achieving efficient charge transport.

Triphenodioxazine (TPDO) (Fig. 1) is the core structure of several commercial dyes and pigments including Pigment Violet 23, 35, 37, and 54 and Direct Blue 104, 106–109, and 190 [14]. Recently, several small molecule TPDO derivatives have been used as

* Corresponding author. Department of Chemical Engineering and Waterloo Institute of Nanotechnology (WIN), University of Waterloo, 200 University Ave West, Waterloo, N2L 3G1, Canada.
** Corresponding author.
E-mail addresses: jinliangw@hotmail.com (J. Wang), yuning.li@uwaterloo.ca (Y. Li).
[1] These authors contributed equally to this work.

http://dx.doi.org/10.1016/j.dyepig.2016.05.011
0143-7208/

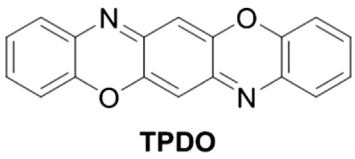

Fig. 1. Chemical structure of benzo[5,6][1,4]oxazino[2,3-*b*]phenoxazine or more commonly known as triphenodioxazine (TPDO).

semiconductors in OPVs [15,16], dye-sensitized solar cells [17], and OTFTs [18–20], showing promising power conversion efficiency of up to 6.3% [17] and electron mobility of up to 0.11 $cm^2 V^{-1} s^{-1}$ [20]. Therefore, it is worthwhile to incorporate the TPDO moiety into polymer semiconductors to explore the optoelectronic properties of the resulting polymers.

In this work we developed a novel TPDO compound, **FTPDO**, which contains a TPDO core fused with two fluorene units (Scheme 1). The purpose of using fluorene units is to allow facile substitution at the 9-positions of fluorenes to render the substituted **FTPDO** compound soluble. In addition, the 7-positions of the fluorene units can be furnished with functional bromo groups allowing **FTPDO** to be used as a comonomer to bithiophene in the Stille coupling reaction to successfully synthesize the polymer **PFTPDOBT** (Scheme 1). This new polymer has a narrow band gap of 1.66 eV and showed remarkable air stability at high temperatures of up to 250 °C. Despite of its poor molecular organization due to the existence of several **FTPDO** isomers, **PFTPDOBT** exhibited promising field effect transistor performance with hole mobility as high as 1.57×10^{-2} $cm^2 V^{-1} s^{-1}$ achieved by annealing the polymer films at 200 °C in air and measuring the devices in air, which is a threefold increase compared to the highest mobility obtained for devices annealed and measured in nitrogen. Our results demonstrate the potential usefulness of **FTPDO** as a new building block for polymer semiconductors for printed organic electronics.

2. Experimental

2.1. Materials and instrumentation

NMR spectra were recorded on a Bruker DPX 300 and 400 MHz spectrometer with chemical resonance signals relative to the residual chloroform in the deuterated solvent (7.26 ppm for ^{1}H NMR and 77 ppm for ^{13}C NMR). Gel-permeation chromatography (GPC) measurements were performed on a Malvern SEC system using 1,2,4-trichlorobenzene as eluent and polystyrene as standards at 140 °C. DSC measurements were carried out on a TA Instruments Q2000 at a temperature ramping rate of 20 °C min^{-1} under nitrogen. The UV–Vis–NIR absorption spectra of the polymer were recorded on a Thermo Scientific GENESYS™ 10S VIS spectrophotometer. Cyclic voltammetry (CV) data were obtained on a CHI600E electrochemical analyzer using an Ag/AgCl reference electrode and two Pt disk electrodes as the working and counter electrodes in a 0.1 M tetrabutylammonium hexafluorophosphate solution in anhydrous acetonitrile at a scan rate of 50 mV s^{-1}. Ferrocene was used as the reference, which has a highest occupied molecular orbital (HOMO) energy level of −4.8 eV [21]. The molecular orbital energies of the monomer and dimer structures were calculated at the Density Functional Theory (DFT) B3LYP/6-31G(d) level and were characterized at the ground/neutral electronic state using the Gaussian 09 Revision D.01 software program [22]. Calculations were performed on model systems of **FTPDO** small molecules and **FTPDOBT** dimers where all side-chain substituents were replaced with methyl groups to reduce computational time. A Bruker D8 Advance powder diffractometer using Cu Kα1 radiation (λ = 1.5406 Å) was used to measure the X-ray diffraction (XRD) patterns of the polymer thin films. The polymer thin film samples were prepared by spin-coating a polymer solution in chloroform on dodecyltrichlorosilane-modified SiO_2/Si substrates and annealed at different temperatures in nitrogen. The same polymer samples were used for obtaining the atomic force microscopy (AFM) images with a Dimension 3100 scanning probe microscope.

2.2. Synthesis of 2-bromo-9,9-dihexadecyl-9H-fluorene (1)

Potassium *tert*-butoxide (15 g, 137 mmol) was added to a stirring solution of 2-bromofluorene (15 g, 61 mmol) in tetrahydrofuran (30 mL) cooled by an ice-water bath. After the addition of potassium *tert*-butoxide, the ice-water bath was removed and the mixture was stirred at room temperature for 40 min. The reaction mixture was once again cooled with an ice-water bath and 1-

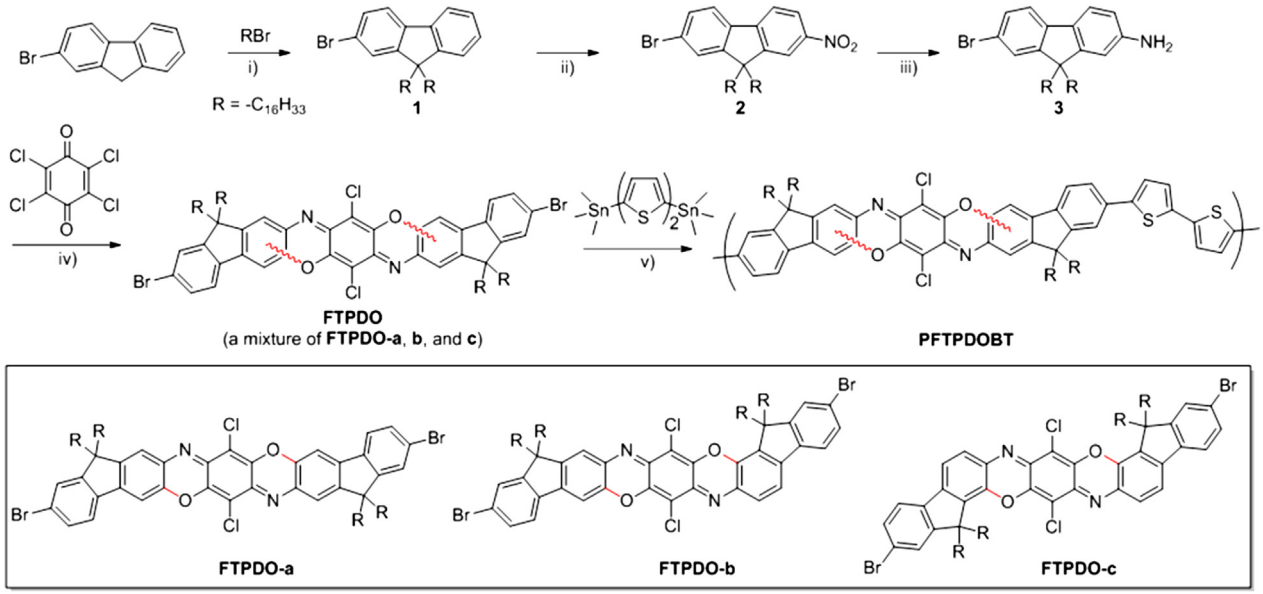

Scheme 1. Synthetic route to **FTPDO** and its polymer **PFTPDOBT**. i) *t*-BuOK, THF, r. t., 80%; ii) 90% HNO_3, 1,2-dichloroethane, reflux, 94%; iii) $NH_2NH_2.H_2O$ (3.0 mL), $Fe(acac)_3$, ethylene glycol, 152 °C, 52%; iv) 4-toluenesulfonylchloride, nitrobenzene, 40 °C, 6%; v) $Pd_2(dba)_3$/P(*o*-tolyl)$_3$), chlorobenzene, 130 °C, 82%.

bromohexadecane (42 g, 138 mmol) was added. The mixture was then stirred at room temperature for 30 min. Water was added to the reaction mixture and the organic phase was separated. With the addition of methanol, a solid precipitated from the organic phase. The precipitate was then collected by filtration and recrystallized with a mixture of methanol and chloroform to afford a yellow solid (34 g, 80% yield). ^{1}H NMR (400 MHz, $CDCl_3$): δ (ppm) 7.67–7.64 (m, 1H), 7.55–7.53 (m, 1H), 7.45–7.42 (m, 2H), 7.33–7.26 (m, 3H), 1.92–1.87 (m, 4H), 1.31–1.07 (m, 56H), 0.87 (t, 6H); ^{13}C NMR (100 MHz, $CDCl_3$): δ (ppm) 153.07, 150.41, 140.26, 140.16, 130.01, 127.57, 127.03, 126.25, 122.96, 121.13, 121.11, 119.86, 55.50, 40.44, 30.14, 29.89, 29.87, 29.83, 29.80, 29.75, 29.73, 29.65, 29.57, 29.41, 28.98, 28.38, 23.84, 22.88, 14.30. The same compound was reported in the literature following an alternative synthetic method [23].

2.3. Synthesis of 2-bromo-9,9-dihexadecyl-7-nitro-9H-fluorene (2)

A mixture of **1** (30 g, 43 mmol), concentrated nitric acid (~90%) (125 mL) and 1,2-dichloroethane (300 mL) was refluxed for 10 h. The reaction mixture was then allowed to cool to room temperature and washed with water until a neutral pH was obtained. The organic phase was collected and dried over anhydrous calcium chloride, filtered and condensed. The condensed solution was added to stirring methanol where a solid quickly precipitated. The precipitate was collected by filtration and recrystallized in methanol to afford a yellow solid (30 g, 94% yield). ^{1}H NMR (400 MHz, $CDCl_3$): δ (ppm) 8.26 (dd, J = 8.4, 2.1 Hz, 1H), 8.18 (d, J = 2.1, 1H), 7.76 (d, J = 8.4 Hz, 1H), 7.64 (d, J = 8.4 Hz, 1H), 7.55–7.51 (m, 2H), 2.09–1.95 (m, 4H), 1.30–1.04 (m, 56H), 0.86 (t, 6H); ^{13}C NMR (100 MHz, $CDCl_3$): δ (ppm) 154.44, 151.66, 147.49, 146.46, 137.79, 130.79, 126.64, 123.79, 123.46, 122.51, 119.98, 118.35, 56.06, 40.05, 32.05, 29.92, 29.84, 29.82, 29.80, 29.78, 29.72, 29.66, 29.62, 29.50, 29.32, 23.83, 22.81, 14.23.

2.4. Synthesis of 7-bromo-9,9-dihexadecyl-9H-fluoren-2-amine (3)

A mixture of **2** (5.0 g, 6.78 mmol), hydrazine hydrate ($NH_2NH_2 \cdot H_2O$) (3.0 mL), iron (III) acetylacetonate ($Fe(acac)_3$) (0.2 g, 0.57 mmol), and ethylene glycol (20 mL) was added into a stainless-steel reaction tube and heated at 155 °C for 2 h. The reaction tube was then cooled and ethyl acetate was added. The ethyl acetate layer was separated and the solvent was removed. The residue was purified by column chromatography (200–300 mesh silica gel with 60–90 petroleum ether: ethyl acetate = 5:1) to afford an orange waxy solid (2.5 g, 52% yield). ^{1}H NMR (400 MHz, $CDCl_3$): δ (ppm) 7.44–7.36 (m, 4H), 6.67–6.62 (m, 2H), 1.87–1.82 (m, 4H), 1.31–1.04 (m, 56H), 0.87 (t, 6H); ^{13}C NMR (100 MHz, $CDCl_3$): δ (ppm) 152.42, 152.17, 146.44, 140.73, 131.41, 129.77, 125.89, 120.73, 119.75, 119.14, 114.16, 109.69, 55.22, 40.68, 32.08, 30.20, 30.12, 29.93, 29.86, 29.84, 29.82, 29.77, 29.74, 29.72, 29.52, 29.45, 23.82, 22.85, 14.27.

2.5. Synthesis of dioxazine derivatives (FTPDO)

A mixture of **3** (2.5 g, 3.53 mmol), sodium carbonate (0.65 g, 6.13 mmol), chloranil (0.63 g, 2.56 mmol), and nitrobenzene (20 mL) was added into a flask and heated at 40 °C for 2 h. 4-Toluenesulfonylchloride (0.86 g, 4.51 mmol) was added into the reaction mixture and the mixture was refluxed for 4 h. Once the reaction mixture was cooled, nitrobenzene was removed at 130 °C *in vacuo* producing a black viscous liquid. The crude product was purified by column chromatography twice (the first column: 100–200 mesh silica gel with 60–90 petroleum ether: ethyl acetate 5:1; the second column: 200–300 mesh silica gel with 60–90 petroleum ether: DMC = 7:1) to afford a dark blue solid (230 mg, 6%). HRMS (ESI^+) calculated for $C_{96}H_{142}Br_2Cl_2N_2O_2$ $(M+H)^+$: 1583.88879 found 1583.89153. The ^{1}H NMR spectrum can be found in Fig. S1 in the Supplementary Data.

2.6. Synthesis of PFTPDOBT

To a 25 mL Schlenk flask, **FTPDO** (110 mg, 0.07 mmol), 5,5′-bis(trimethylstannyl)-2,2′-bithiophene (34 mg, 0.07 mmol) and tri(*o*-tolyl)phosphine ($P(o\text{-tolyl})_3$) (1.7 mg, 0.006 mmol) were added. After degassing and refilling argon three times, chlorobenzene (3 mL) and tris(dibenzylideneacetone)-dipalladium ($Pd_2(dba)_3$) (1.3 mg, 0.001 mmol) were added. The reaction mixture was stirred at 130 °C for 72 h. Upon cooling to room temperature, the reaction mixture was poured into methanol (100 mL). The precipitate was collected by filtration and subject to Soxhlet extraction with acetone, hexanes, and chloroform successively. The residue was dissolved in chloroform to give **PFTPDOBT** upon removal of solvent in *vacuo*. Yield: 90 mg (82%). GPC data: M_n = 15,432; PDI = 2.64. The ^{1}H NMR spectrum can be found in Fig. S2 in the Supplementary Data.

2.7. Fabrication and characterization of organic thin film transistors (OTFTs)

A bottom-gate bottom-contact (BGBC) configuration was used for all OTFT devices. The device fabrication procedure is as follows. A heavily n^{++}-doped SiO_2/Si wafer with a ~300 nm-thick SiO_2 layer was patterned with gold source and drain pairs by conventional photolithography and thermal deposition techniques. Subsequently, the substrate was treated with O_2-plasma, followed by cleaning with acetone and then isopropanol in an ultra-sonicating bath. Then the substrate was placed in a solution of dodecyltrichlorosilane in toluene (10 mg mL^{-1}) at room temperature for 20 min, followed by washing with toluene and drying under a nitrogen flow. A polymer solution in chloroform (5 mg mL^{-1}) was spin-coated onto the substrate at 3000 rpm for 60 s to give a polymer film (~40 nm), which was further subject to thermal annealing at various temperatures for 30 min in a glove box filled with nitrogen or in air (with a relative humidity of 45%). All the OTFT devices have a channel length (L) of 30 μm and a channel width (W) of 1000 μm. Devices were characterized in the same glove box or in air in dark using an Agilent B2912A Precision Source/Measure Unit. The reported mobility (μ) values were calculated using the saturated regime current-voltage characteristics with the drain-source current (I_{DS}) given by:

$$I_{DS} = \left(\frac{WC_i}{2L}\right)\mu(V_G - V_T)^2$$

where C_i is the capacitance per unit area of the dielectric (11.6 nF cm^{-2}), W and L are OTFT channel width and length, V_G is the gate voltage, and V_T is the threshold voltage.

3. Results and discussion

The new f. luorene-fused TPDO compound, **FTPDO**, and its polymer **PFTPDOBT** were prepared according to the synthetic route outlined in Scheme 1. 2-Bromofluorene was first disubstituted at the 9-position with hexadecyl groups, followed by nitration at the 5-position, producing compound **2**. Reduction of **2** with hydrazine hydrate in the presence of iron (III) acetylacetonate ($Fe(acac)_3$) as a catalyst in ethylene glycol at 155 °C afforded the key amino fluorene compound **3**, which was reacted with chloranil to form the target **FTPDO**. Because the ring closure could occur at the 6- or 8-position of a fluorene unit, three possible isomers, **FTPDO-a**, **b**, and **c**, might form (shown in the insert of Scheme 1). Thin layer chromatography

(TLC) analysis indeed showed three overlapped spots, but the separation of these three compounds was not successful due to their very similar polarity. Nonetheless, since all three isomers of **FTPDO** have fully π-conjugated pathways between the two C–Br groups, they would form extended main chain conjugation if they are incorporated in the polymer backbone. Therefore, the mixture of **FTPDO-a**, **b**, and **c** was used as a comonomer to 5,5-bis(trimethylstannyl)-2,2′-bithiophene to form the polymer **PFTPDOBT** under typical Stille coupling polymerization conditions in the presence of $Pd_2(dba)_3$/P(*o*-tolyl)$_3$ as a catalyst in chlorobenzene at 130 °C for 72 h. The resulting polymer was precipitated from methanol and further purified by Soxhlet extraction using acetone, hexane, and chloroform. The polymer fraction dissolved by chloroform was dried to give the final polymer product in 82% yield.

GPC was used to characterize the molecular weight of **PFTPDOBT** using 1,2,4-trichlorobenzene as an eluent at a column temperature of 140 °C. The number-average molecular weight (M_n) and polydispersity index (PDI) were determined to be 15.4 kmol g^{-1} and 2.64, respectively, relative to the polystyrene standards (Fig. S3). **PFTPDOBT** showed a λ_{max} at 649 nm and a shoulder at ~670 nm in a chloroform solution. The polymer thin film spin-coated on a glass substrate showed a λ_{max} at 673 nm and a minor peak at ~620 nm (Fig. 2a). The optical band gap calculated from the onset absorption of the polymer film is 1.66 eV. The cyclic voltammetry (CV) curves of the polymer film showed strong oxidation peaks, but no obvious reduction peaks (Fig. 2b). The HOMO energy level of **PFTPDOBT** is obtained from its oxidation onset potential using ferrocene (Fc) ($E_{HOMO,\ Fc} = -4.8$ eV) as a reference to be −5.61 eV. The lowest unoccupied molecular orbital (LUMO) energy level is estimated from the HOMO and the optical band gap to be −3.95 eV. The rather low HOMO and LUMO energy levels of **PFTPDOBT** suggest that **FTPDO** is a strong electron withdrawing building block. The narrow band gap of this polymer can be attributed to the intramolecular charge transfer from the donor (bithiophene) to the acceptor (the TPDO core).

The calculated frontier energy levels for the isomeric **FTPDO-a**, **b** and **c** monomer units display similar characteristics and have energies within a narrow range of −3.04 to −3.08 eV for LUMO and −5.20 to −5.28 eV for HOMO (Fig. 3). Interestingly, both the LUMO and HOMO energy levels decrease by intervals of 0.02 and 0.04 eV, respectively, from **FTPDO-a** to **FTPDO-c**, suggesting that the LUMO and HOMO energy levels are only slightly affected by the different placement of the fluorene moiety fused to the TPDO core. Compared with the **FTPDO-a**, **b** and **c** monomer units, the calculated frontier energy levels for **FTPDOBT-a**, **b** and **c** dimers displayed only a minor increase in LUMO energy levels ranging from −2.95 to −2.97 eV, while the HOMO energy levels increased notably as expected with the addition of the bithiophene donor, ranging from −4.90 to −4.95 eV. For each dimer, the LUMO wavefunction localizes onto the **FTPDO** moiety and is more influenced by the electron-accepting nature of the acceptor, whereas the HOMO wavefunction is more delocalized along the dimer backbone and only marginally affected by the acceptor characteristics (see Figs. S5–S7 in Supplementary Data).

The TGA profile of **PFTPDOBT** under nitrogen showed the 5% weight loss at a temperature of 354 °C (Fig. S8), indicating that this polymer is quite thermally stable. Differential scanning calorimetry (DSC) measurement did not show any obvious thermal transition in a temperature range between 25 °C and 300 °C (Fig. S9). To determine the molecular ordering or crystallinity, **PFTPDOBT** films were prepared by spin-coating a polymer solution in chloroform on SiO_2/Si substrates and annealed at 100 °C for 15 min under nitrogen, which were subject to XRD measurements. No distinct reflection peak was observed, suggesting the polymer film annealed at this temperature is amorphous (Fig. 4). Once the annealing temperature is increased to 150 °C, a weak diffraction peak appeared at 2θ = ~4°, which corresponds to a *d*-spacing of 2.21 nm. Further increasing the annealing temperature intensifies this diffraction peak. However, the intensity of this peak is still very weak even at a high annealing temperature of 250 °C. The poor molecular organization of this polymer is most likely due to the existence of three isomeric **FTPDO** units (Scheme 1), which results in kinked polymer main chains, hampering the formation of ordered chain packing [24]. The morphology changes of the polymer films with annealing temperature were characterized by AFM (Fig. 5). The 100 °C- and 150 °C-annealed films are quite smooth with a small square root roughness (R_q) of 0.6 nm. Once the annealing temperature is increased to 200 °C, large grains begin to appear and the film becomes rougher (R_q = 1.2 nm). The grain size further grows as the temperature increases to 250 °C, which is accompanied with the increased crystallinity of the film verified by the XRD data.

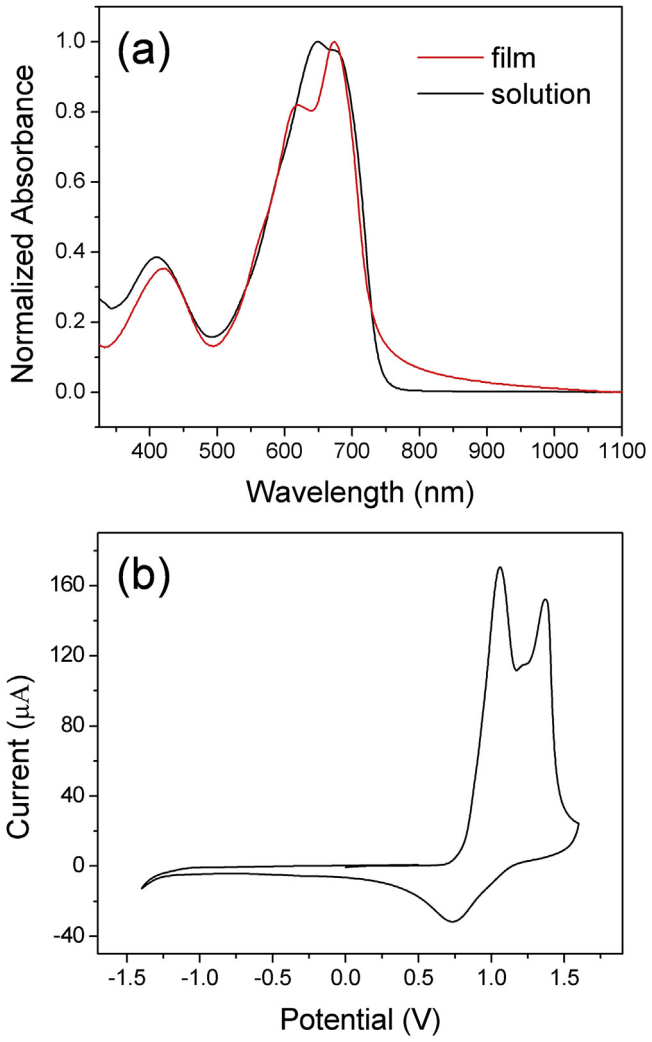

Fig. 2. (a) UV–Vis spectra and (b) cyclic voltammogram of **PFTPDOBT**.

PFTPDOBT was evaluated as a channel semiconductor in bottom-gate bottom-contact OTFT devices (Fig. 6a). A solution of **PFTPDOBT** in chloroform was spin-coated on a dodecyltrichlorosilane modified SiO_2/n^{++}-Si wafer substrate with pre-patterned Au source and drain pairs and annealed at different temperatures for 15 min in a glove box filled with nitrogen. All devices showed typical p-channel field effect transistor

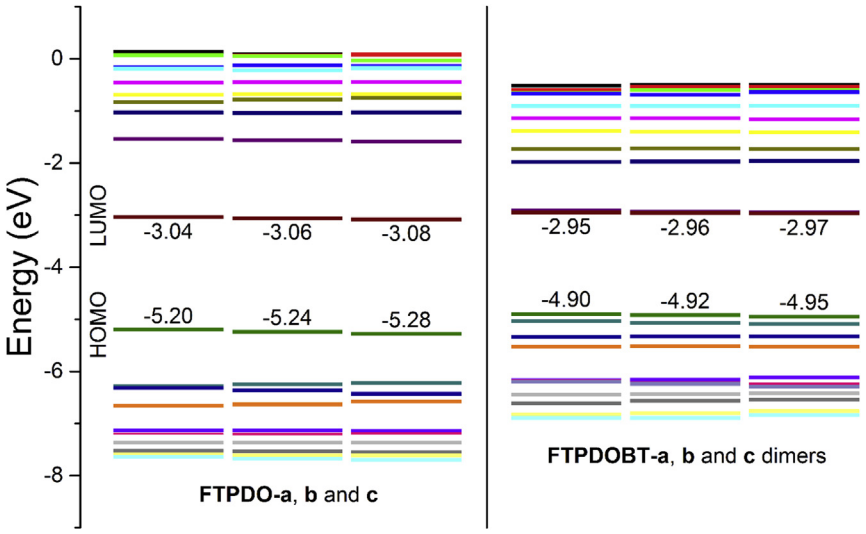

Fig. 3. The molecular orbital energies (±10 from LUMO and HOMO) for **FTPDO-a**, **b** and **c** and **FTPDOBT-a**, **b** and **c** dimers (see Supplementary Data for their chemical structures).

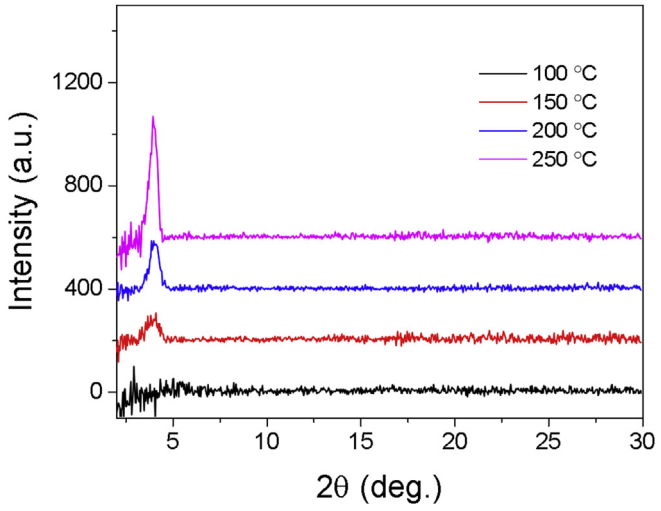

Fig. 4. XRD patterns of **PFTPDOBT** films spin-coated on dodecyltrichlorosilane-modified Si/SiO_2 substrates annealed at different temperatures.

temperatures showed significant improvements in the hole mobilities (Figs. 6 and 7 and Table S2). The highest mobility of 1.44×10^{-2} cm^2 V^{-1} s^{-1} was obtained for a device with the polymer film annealed at 200 °C (Fig. 6b). To further study the influence of air on the charge transport performance of this polymer, the polymer thin films were annealed in air at different temperatures ranging from 50 °C to 250 °C and tested in air. Unexpectedly, the average mobilities increased further at all annealing temperatures (Figs. 6 and 7 and Table S3). The highest mobility of 1.57×10^{-2} cm^2 V^{-1} s^{-1} was achieved at an annealing temperature of 200 °C (Fig. 6c). It appears that oxygen, moisture, or some other component in air promoted the device performance. To investigate if the polymer is intact after annealing in air, the polymer films annealed in nitrogen or air were characterized by UV–Vis spectrometry. The absorption profiles and the λ_{max} of the polymer films annealed in nitrogen or air are very similar at all respective annealing temperatures (Figs. S10 and S11). In both environments, the λ_{max} increases with annealing temperature, which was associated with the increased molecular ordering as evidenced by the XRD measurement. Based on the above UV–Vis study, it seems that

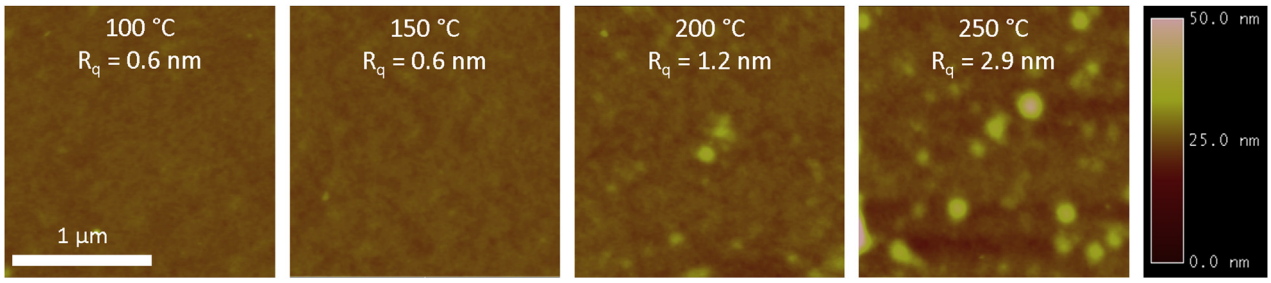

Fig. 5. AFM images (2 μm × 2 μm) of **PFTPDOBT** films spin-coated on dodecyltrichlorosilane-modified Si/SiO_2 substrates annealed at different temperatures.

performance (Figs. 6 and 7 and Table S1). The best hole mobility of 5.27×10^{-3} cm^2 V^{-1} s^{-1} was obtained for a device annealed at 200 °C (Fig. 6b and Table S1). To evaluate the air stability of this polymer under operation, the devices were characterized in air (with a relative humidity of 45%) with the polymer semiconductor layer exposed to air. Surprisingly, the devices at all annealing air had minimal influences on this polymer at an annealing temperature up to 250 °C. It should be noted that when the devices measured in air were transferred into the nitrogen-filled glove box for re-testing, the mobilities decreased compared to the values measured in air. Once the devices were taken out of the glove box and measured again in air, the mobilities recovered. Reproducible

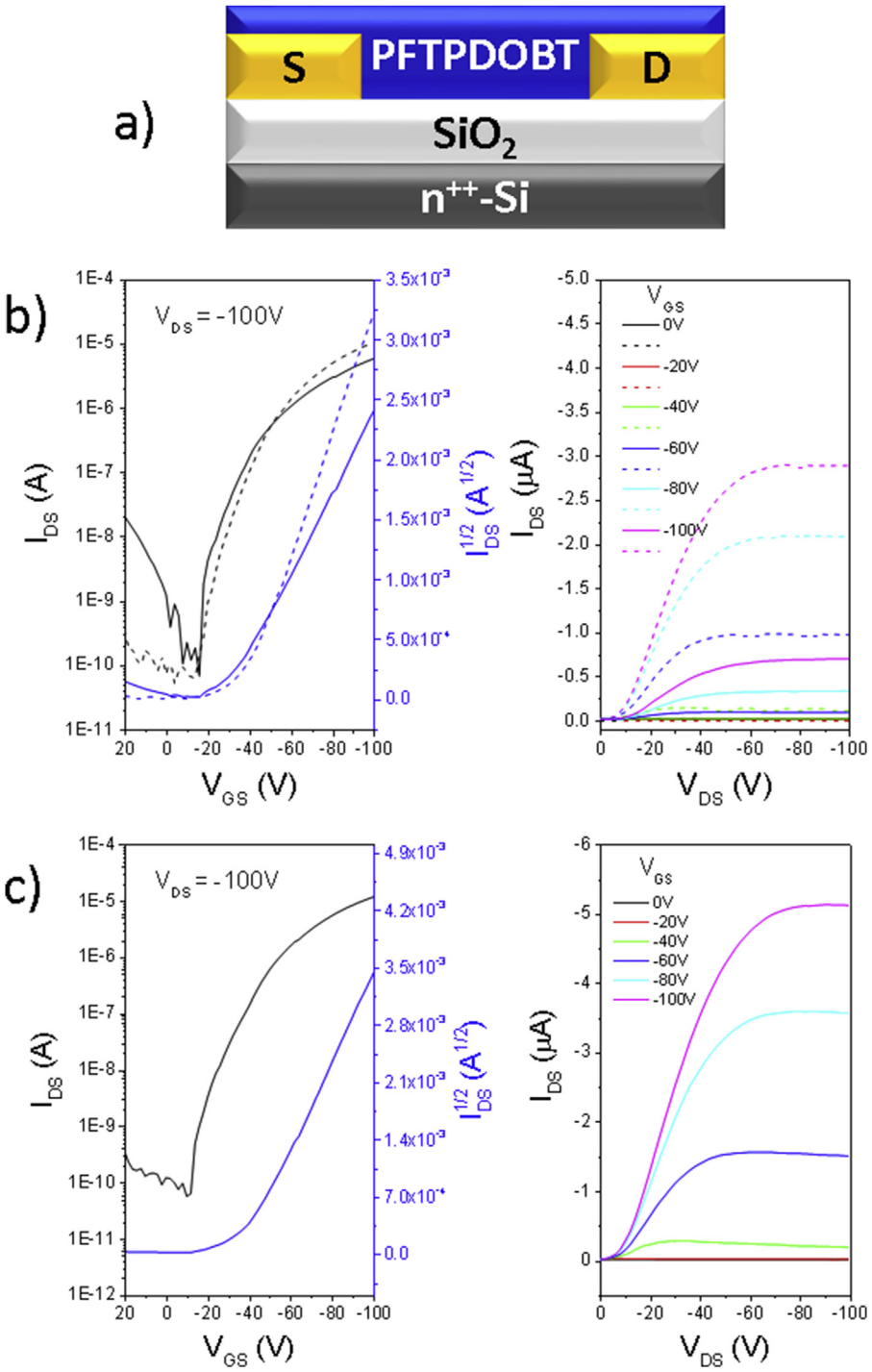

Fig. 6. a) Bottom-gate bottom-contact (BGBC) OTFT structure used for the evaluation of **PFTPDOBT**. b) Transfer (left) and output (right) characteristics of an OTFT device with a **PFTPDOBT** film annealed at 200 °C in nitrogen and tested in nitrogen (solid lines) and air (dashed lines). c) Transfer (left) and output (right) characteristics of an OTFT device with a **PFTPDOBT** film annealed at 200 °C in air and tested in air. Device dimensions: channel length = 30 μm; channel width = 1000 μm.

results were obtained when this process was repeated. The stability of polymer semiconductors at high temperatures in air is very important for device manufacturing because it allows the annealing step to be conducted in air, which facilitates the roll-to-roll high throughput production of printed electronics. The reason for the marked enhancement of the device performance of the polymer films annealed and/or measured in air is still unclear. One possible reason might be the interaction of oxygen with the Au source and drain contacts. A previous study showed that the work function of gold increased from 4.7–4.9 eV to 5.0–5.5 eV, which could reduce the hole injection barrier from the Au source to the polymer semiconductor layer [25]. The effect might be particularly prominent for this polymer because its HOMO energy level is rather low (−5.61 eV).

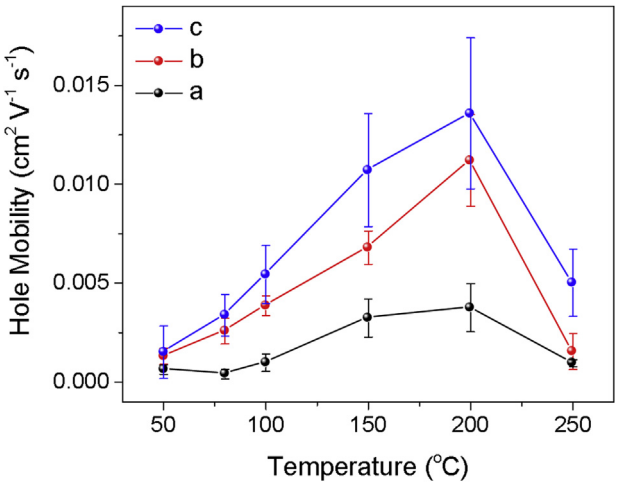

Fig. 7. The hole mobilities of BGBC OTFT devices with **PFTPDOBT** films at different annealing temperatures: a) polymer films annealed in nitrogen and devices tested in nitrogen, b) polymer films annealed in nitrogen and devices tested in air, and c) polymer films annealed in air and devices tested in air. Device dimensions: channel length = 30 μm; channel width = 1000 μm.

4. Conclusion

In conclusion, a novel electron acceptor building block, fluorene-fused triphenodioxazine (**FTPDO**), and a donor-acceptor polymer based on **FTPDO** and bithiophene, **PFTPDOBT**, are reported. This new polymer showed good hole transport performance with hole mobilities of up to 1.57 × 10^{-2} cm^2 V^{-1} s^{-1} in organic thin film transistors despite of its poor molecular ordering due to the existence of several isomeric **FTPDO** units. Particularly important is that the highest device performance was achieved by annealing the polymer films and testing the devices in air. The excellent air stability, good charge transport performance, and narrow band gap (1.66 eV) make the **FTPDO**-based polymers promising for stable printed electronics where air exposure during the manufacturing and operation of these electronics is inevitable. The charge transport performance is expected to improve if an isomerically pure **FTPDO** monomer can be isolated or synthesized, which is the subject of our next step study on this new class of polymers.

Acknowledgments

This work is partially supported by the Natural Sciences and Engineering Research Council (NSERC) of Canada (Discovery Grant #402566-2011).

Appendix A. Supplementary data

Supplementary data related to this article can be found at http://dx.doi.org/10.1016/j.dyepig.2016.05.011.

References

[1] Facchetti A. π-Conjugated polymers for organic electronics and photovoltaic cell applications †. Chem Mater 2011;23:733–58. http://dx.doi.org/10.1021/cm102419z.
[2] Günes S, Neugebauer H, Sariciftci NS. Conjugated polymer-based organic solar cells. Chem Rev 2007;107:1324–38. http://dx.doi.org/10.1021/cr050149z.
[3] Arias AC, MacKenzie JD, McCulloch I, Rivnay J, Salleo A. Materials and applications for large area electronics: solution-based approaches. Chem Rev 2010;110:3–24. http://dx.doi.org/10.1021/cr900150b.
[4] Klauk H. Organic thin-film transistors. Chem Soc Rev 2010;39:2643. http://dx.doi.org/10.1039/b909902f.
[5] Li Y, Sonar P, Murphy L, Hong W. High mobility diketopyrrolopyrrole (DPP)-based organic semiconductor materials for organic thin film transistors and photovoltaics. Energy Environ Sci 2013;6:1684. http://dx.doi.org/10.1039/c3ee00015j.
[6] Nielsen CB, Turbiez M, McCulloch I. Recent advances in the development of semiconducting DPP-containing polymers for transistor applications. Adv Mater 2013;25:1859–80. http://dx.doi.org/10.1002/adma.201201795.
[7] Irimia-Vladu M, Głowacki ED, Troshin PA, Schwabegger G, Leonat L, Susarova DK, et al. Indigo - a natural pigment for high performance ambipolar organic field effect transistors and circuits. Adv Mater 2012;24:375–80. http://dx.doi.org/10.1002/adma.201102619.
[8] Guo C, Sun B, Quinn J, Yan Z, Li Y. Synthesis and properties of indigo based donor–acceptor conjugated polymers. J Mater Chem C 2014;2:4289. http://dx.doi.org/10.1039/c3tc32276a.
[9] Guo C, Quinn J, Sun B, Li Y. An indigo-based polymer bearing thermocleavable side chains for n-type organic thin film transistors. J Mater Chem C 2015;3:5226–32. http://dx.doi.org/10.1039/C5TC00512D.
[10] Guo C, Quinn J, Sun B, Li Y. Regioisomeric control of charge transport polarity for indigo-based polymers. Polym Chem 2015;6:6998–7004. http://dx.doi.org/10.1039/C5PY00821B.
[11] Lei T, Cao Y, Fan Y, Liu C-J, Yuan S-C, Pei J. High-performance air-stable organic field-effect transistors: isoindigo-based conjugated polymers. J Am Chem Soc 2011;133:6099–101. http://dx.doi.org/10.1021/ja111066r.
[12] Mei J, Kim DH, Ayzner AL, Toney MF, Bao Z. Siloxane-terminated solubilizing side chains: bringing conjugated polymer backbones closer and boosting hole mobilities in thin-film transistors. J Am Chem Soc 2011;133:20130–3. http://dx.doi.org/10.1021/ja209328m.
[13] Lei T, Dou J-H, Pei J. Influence of alkyl chain branching positions on the hole mobilities of polymer thin-film transistors. Adv Mater 2012;24:6457–61. http://dx.doi.org/10.1002/adma.201202689.
[14] Renfrew AHM. Reactive dyes for cellulose: replacement of anthraquinone blues by triphenodioxazines. Rev Prog Color Relat Top 1985;15:15–20. http://dx.doi.org/10.1111/j.1478-4408.1985.tb03731.x.
[15] Yoshida S, Kozawa K, Uchida T. Photovoltaic properties of triphenodioxazine and dichlorotriphenodioxazine. Bull Chem Soc Jpn 1995;68:738–43. http://dx.doi.org/10.1246/bcsj.68.738.
[16] Qiao F, Liu A, Xiao Y, Ou YP, Zhang JQ, Sang YC. Enhanced photovoltaic characteristics of solar cells based on n-type triphenodioxazine derivative. Microelectron J 2008;39:1568–71. http://dx.doi.org/10.1016/j.mejo.2008.02.027.
[17] Nicolas Y, Allama F, Lepeltier M, Massin J, Castet F, Ducasse L, et al. New synthetic routes towards soluble and dissymmetric triphenodioxazine dyes designed for dye-sensitized solar cells. Chem Eur J 2014;20:3678–88. http://dx.doi.org/10.1002/chem.201303775.
[18] Di C, Li J, Yu G, Xiao Y, Guo Y, Liu Y, et al. Trifluoromethyltriphenodioxazine: air-stable and high-performance n-type semiconductor. Org Lett 2008;10:3025–8. http://dx.doi.org/10.1021/ol8008667.
[19] Nicolas Y, Castet F, Devynck M, Tardy P, Hirsch L, Labrugère C, et al. TIPS-triphenodioxazine versus TIPS-pentacene: enhanced electron mobility for n-type organic field-effect transistors. Org Electron 2012;13:1392–400. http://dx.doi.org/10.1016/j.orgel.2012.04.010.
[20] Gruntz G, Lee H, Hirsch L, Castet F, Toupance T, Briseno AL, et al. Nitrile substitution effect on triphenodioxazine-based materials for liquid-processed air-stable n-type organic field effect transistors. Adv Electron Mater 2015;1. http://dx.doi.org/10.1002/aelm.201500072. n/a – n/a.
[21] Pommerehne J, Vestweber H, Guss W, Mahrt RF, Bässler H, Porsch M, et al. Efficient two layer leds on a polymer blend basis. Adv Mater 1995;7:551–4. http://dx.doi.org/10.1002/adma.19950070608.
[22] Frisch MJ, Trucks GW, Schlegel HB, Scuseria GE, Robb MA, Cheeseman JR, et al. Gaussian 09 revision D.01. Wallingford, CT, USA: Gaussian, Inc.; 2009.
[23] Liu L, Wong W-Y, Lam Y-W, Tam W-Y. Exploring a series of monoethynyl-fluorenes as alkynylating reagents for mercuric ion: synthesis, spectroscopy, photophysics and potential use in mercury speciation. Inorg Chim Acta 2007;360:109–21. http://dx.doi.org/10.1016/j.ica.2006.07.037.
[24] Osaka I, Abe T, Shinamura S, Takimiya K. Impact of isomeric structures on transistor performances in naphthodithiophene semiconducting polymers. J Am Chem Soc 2011;133:6852–60. http://dx.doi.org/10.1021/ja201591a.
[25] Chen Z, Lee MJ, Shahid Ashraf R, Gu Y, Albert-Seifried S, Meedom Nielsen M, et al. High-performance ambipolar diketopyrrolopyrrole-thieno[3,2- *b*]thiophene copolymer field-effect transistors with balanced hole and electron mobilities. Adv Mater 2012;24:647–52. http://dx.doi.org/10.1002/adma.201102786.